

**An Underwater Acoustic Source for the  
Infrasonic and Low-Audio-Frequency Range  
(USRD Type J13 Transducer)**

A. MARK YOUNG

*Standards Branch  
Underwater Sound Reference Division*

30 December 1975

**PLEASE RETURN THIS COPY TO:**

**NAVAL RESEARCH LABORATORY  
WASHINGTON, D. C. 20375  
ATTN: CODE 2628**

Because of our limited supply you are requested to return this copy as soon as it has served your purposes so that it may be made available to others for reference use. Your cooperation will be appreciated.

NDW-NRL-5070/2651 (Rev. 9-75)



**NAVAL RESEARCH LABORATORY  
Underwater Sound Reference Division  
P. O. Box 8337, Orlando, Fla. 32806**

Approved for public release; distribution unlimited.

## REPORT DOCUMENTATION PAGE

READ INSTRUCTIONS  
BEFORE COMPLETING FORM

1. REPORT NUMBER NRL Report 7967		2. GOVT ACCESSION NO.	3. RECIPIENT'S CATALOG NUMBER
4. TITLE (and Subtitle) AN UNDERWATER ACOUSTIC SOURCE FOR THE INFRASONIC AND LOW-AUDIO-FREQUENCY RANGE (USRD TYPE J13 TRANSDUCER)		5. TYPE OF REPORT & PERIOD COVERED Final report on one part of the problem.	
7. AUTHOR(s) A. Mark Young		6. PERFORMING ORG. REPORT NUMBER	
9. PERFORMING ORGANIZATION NAME AND ADDRESS Naval Research Laboratory Underwater Sound Reference Division P.O. Box 8337, Orlando, Fla. 32806		8. CONTRACT OR GRANT NUMBER(s)	
11. CONTROLLING OFFICE NAME AND ADDRESS Department of the Navy Office of Naval Research Arlington, Va. 22217		10. PROGRAM ELEMENT, PROJECT, TASK AREA & WORK UNIT NUMBERS NRL Problem S02-31 Project RF-11-121-403--4472	
14. MONITORING AGENCY NAME & ADDRESS (if different from Controlling Office)		12. REPORT DATE 30 December 1975	
		13. NUMBER OF PAGES ii + 19	
		15. SECURITY CLASS. (of this report) Unclassified	
		15a. DECLASSIFICATION/DOWNGRADING SCHEDULE	
16. DISTRIBUTION STATEMENT (of this Report)  Approved for public release; distribution unlimited.			
17. DISTRIBUTION STATEMENT (of the abstract entered in Block 20, if different from Report)			
18. SUPPLEMENTARY NOTES			
19. KEY WORDS (Continue on reverse side if necessary and identify by block number) Electrodynamic acoustic transducer Low-audio-frequency transducer Transducer design Transducer construction Underwater acoustic transducer			
20. ABSTRACT (Continue on reverse side if necessary and identify by block number)  An electrodynamically driven underwater sound source with an acoustic output of 1.349 W has been developed. Adapted in various configurations including as many as nine driving units, this transducer fulfills a substantial portion of the needs for low-audio-frequency underwater sound sources.			

## Contents

Introduction . . . . .	1
Design Considerations . . . . .	2
Construction . . . . .	4
Analysis . . . . .	7
Conclusions . . . . .	11
Acknowledgments . . . . .	11
References . . . . .	11
Appendix A. Determination of Values for Elements of the J13 Equivalent Circuit . . . . .	12

## Figures

1. USRD electrodynamic transducers types J9, J11, and J13 . . . . .	1
2. Summary of design considerations . . . . .	5
3. Sectional view of USRD type J13 transducer . . . . .	6
4. Equivalent circuit for USRD type J13 transducer, classical analogy . . . . .	7
5. Equivalent circuit for USRD type J13 transducer, mobility analogy . . . . .	8
6. Equivalent circuit for USRD type J13 transducer, mobility analogy for electronic circuit analysis by time-sharing computer program . . . . .	9
7. Comparison of USRD type J13 transmitting current response data obtained by measurement with results from equivalent circuit calculations . . . . .	10

## Table

1. Some operating characteristics of USRD type J9, J11, and J13 transducers . . . . .	2
--	---

AN UNDERWATER ACOUSTIC SOURCE FOR THE  
INFRASONIC AND LOW-AUDIO-FREQUENCY RANGE  
(USRD Type J13 TRANSDUCER)

Introduction

About twenty years ago, the Underwater Sound Reference Division developed the first in a series of broadband, electro-dynamically driven sound sources for the audio-frequency range, the USRD type J9 transducer, which was intended primarily for use as a calibration source. Within less than ten years after the J9 was introduced, the requirements for a more powerful sound projector prompted development of a somewhat larger transducer designated USRD type J11. Ever since the time they were developed, both of these transducers have been used extensively in laboratory and ocean applications.

Growing interest in at-sea calibration during the late 1960's and early 1970's stimulated development of the USRD type J13 infrasonic and low-audio frequency transducer, which is capable of radiating more power at lower frequencies than either of the two predecessors. Although the designs of the J9, J11, and J13 transducers are based on the same operating principles, unique features of the J13 provide significantly greater power and adaptability. The three transducers are compared briefly in Fig. 1 and Table 1.

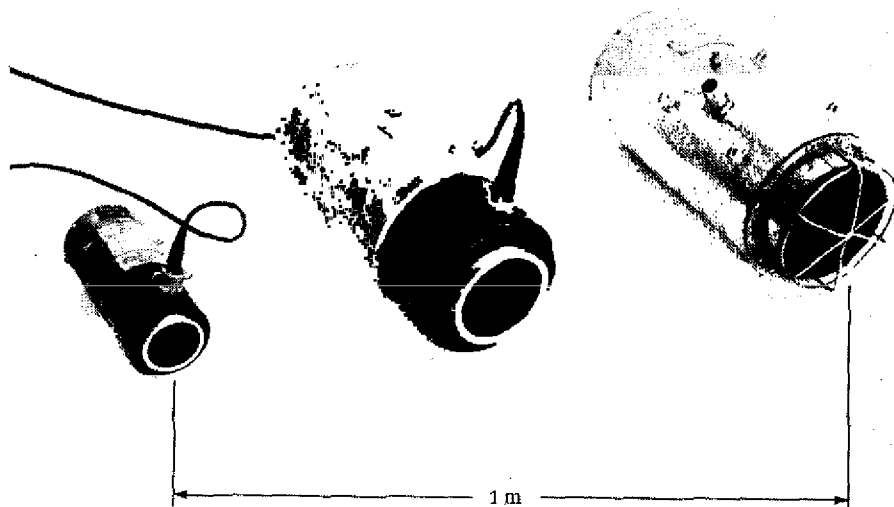


Fig. 1. USRD electrodynamic transducers types J9, J11, and J13 (left to right).

Table 1. Some operating characteristics of USRD transducers types J9, J11, and J13.

USRD transducer type	Freq range (kHz)	Max electr input power (W)	Max acoust output power (W)	Weight in air (kg)
J9	0.04-20	20	0.013	9
J11	0.02-12	200	0.269	46
J13	0.01-3	250	1.349	55

### Design Considerations

The primary design goals for the J13 transducer were:

- a. Maximum useful bandwidth in the infrasonic and low-audio frequency range.
- b. Maximum acoustic output for the smallest possible size and lightest weight.

The parameters affecting these goals are best understood by inspection of the fundamental equations for an electrodynamically driven piston at the end of a long tube.

The bandwidth in which the transducer may provide a flat response is bounded on the low end by the frequency  $\omega_0$  at which the total mass  $M_T$  resonates with the total system compliance  $C_T$  so that

$$\omega_0 = (1/C_T M_T)^{1/2}. \quad (1)$$

The upper limit of this band is that frequency above which the diaphragm no longer moves as a piston; that is, the phase across the diaphragm face is no longer constant. This frequency is a function of the geometrical shape and dimensions of the diaphragm and of the material from which it is made.

Equations describing the output acoustic pressure from a circular piston at the end of a long tube in terms of electrical input parameters and as a function of frequency have been developed by Sims and others [1,2,3]. For a piston operating above the resonance frequency  $\omega_0$ , the transmitting current response measured at a distance of one meter may be represented by

$$\frac{p}{i} = \left( \frac{(Bl)^2 \rho_0 c_0 R_R}{4\pi [R_R^2 + (\omega M_d + X_R)^2]} \right)^{1/2}, \quad (2)$$

where  $p$  is the acoustic pressure at one meter,  $i$  is the driving current,  $B$  is the flux density in the gap of the magnet,  $\ell$  is the length of the conducting coil interacting with  $B$ ,  $\rho_0$  is the density of water,  $c_0$  is the speed of sound in water,  $R_0$  is the directivity factor,  $R_R$  is the series radiation resistance,  $\omega$  is the angular frequency,  $M_d$  is the mass of the diaphragm, and  $X_R$  is the series radiation reactance.

Equation (2) may be rewritten as the acoustic pressure at one meter:

$$p = B\ell i \left[ \frac{\rho_0 c_0 R_0 R_R}{4\pi [R_R^2 + (\omega M_d + X_R)^2]} \right]^{1/2} \quad (3)$$

Relative effects of the design parameters become evident upon inspection of the preceding equations: bandwidth can be increased by reducing the resonance frequency and increasing the stiffness-to-mass ratio of the diaphragm; the acoustic output can be increased by increasing the force factor  $B\ell i$  and decreasing the total effective mass. It is readily apparent that some of these requirements are contradictory: the first goal suggests that the total mass be increased, but the second goal requires that the mass be decreased.

The flux density in the gap of the magnet is determined primarily by the type of magnetic material used and the ratio of its volume to that of the gap. The maximum length of coil conductor (more correctly the maximum product of  $\ell$  and  $i$ ) is limited by the volume of the gap and the maximum allowable input electrical power, which is largely controlled by the rate of heat dissipation from the driving coil.

The total mass is comprised of the diaphragm mass and the mass reactance due to the water load, the latter being a function of the diaphragm radius  $a$  and the medium; therefore, a large portion of the total mass (in many cases the largest portion) is fixed when the diaphragm radius is chosen and becomes unavailable as a parameter to be compromised by design.

For a source whose size is small in comparison with a wavelength in the propagating medium, it can be shown that the radiated acoustic power is determined by the radiation resistance acting on, and the volume velocity generated by, the source [4]. Radiation resistance, like radiation reactance, depends upon the diaphragm radius and the medium, and it is also directly proportional to the square of the frequency; therefore, to maintain a constant output with decreasing frequency, the volume velocity must increase at the same rate that the radiation resistance decreases. From the definition of volume velocity as the product of the radiator surface area and the velocity of that surface, it is seen that the surface displacement is inversely proportional to the square of the frequency and that there is a minimum frequency at which the maximum acoustic output occurs. This frequency is determined by the maximum

allowable displacement of the diaphragm and is computed from

$$\omega = 2(pr/\xi\rho_0)^{1/2}/a, \quad (4)$$

where  $p$  is the sound pressure measured at distance  $r$  when using maximum electrical input, and  $\xi$  is the maximum allowable root mean square displacement of a diaphragm whose radius is  $a$ . At lower frequencies, the sound pressure generated is proportional to the radiation resistance and is, therefore, decreasing at 12 dB per octave.

Oposing requirements are also found at the periphery of the piston. The high radiation impedance of the medium acting on the piston requires maintaining high acoustic impedance in the vicinity of the diaphragm; any areas of low acoustic impedance permit power to be "shunted" past the piston. Thus, the piston suspension must be mechanically compliant to maintain the low resonance frequency and allow for large piston displacement, but must present a high acoustic impedance to the surrounding medium.

A further design consideration related to the resonance frequency and, therefore, to the output at low frequencies, is the depth-compensation or pressure-release system. A most effective pressure release for highly compliant systems is provided by a gas compensation system; however, such systems are prone to performance problems. In Eq. (1) the total mass  $M_T$  is the sum of the diaphragm mass and the mass reactance of the water load, and the total compliance  $C_T$  is the effective net compliances of the diaphragm suspension and the volumes contained in the compensation system. The diaphragm mass, radiation mass, and suspension compliance are all independent of the ambient hydrostatic pressure. If it is assumed that there is a rigid-walled chamber behind the piston, however, the compliance of the gas system is given by

$$C = p_0 V_0 / \gamma p^2, \quad (5)$$

where  $p_0$  and  $V_0$  are the initial gas pressure and volume, respectively,  $\gamma$  is the ratio of the specific heats of the gas at the two pressures, and  $p$  is the pressure at the operating depth. Equations (1) and (5) show that the resonance frequency is proportional to depth; this effect can be minimized for a given maximum operating depth, but it cannot be eliminated.

The maximum operating depth attainable with this type of compensation is determined by the residual volume behind the piston and the total available volume of compensation gas.

Figure 2 graphically summarizes the major design considerations that have been discussed.

## Construction

The USRD type J13 transducer represents the end product of a series

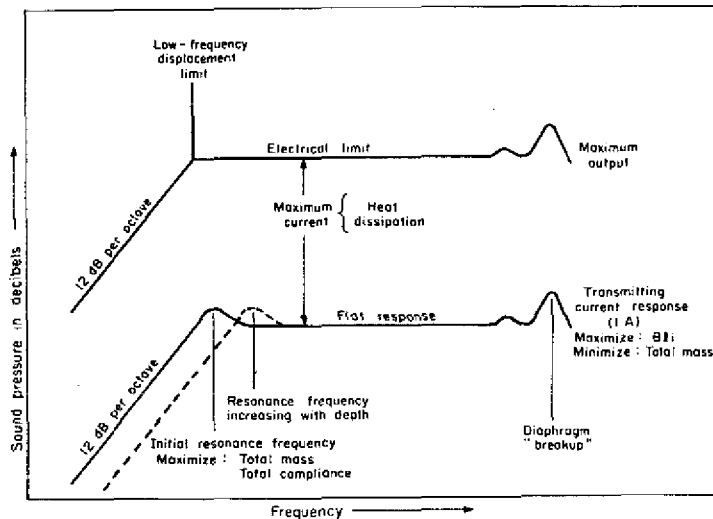


Fig. 2. Summary of design considerations.

of design compromises between the many contradictory requirements outlined in the preceding discussion. Figure 3 shows the most important features of the J13 referred to in the functional description that follows.

Flux density in the gap of the magnet is generated by one 3.6-kg Alnico 5-7 magnet and three Armco copper-plated magnetic iron pole pieces. Spurious resonances in the magnet assembly are damped by filling voids with a matrix of lead shot and epoxy cement. The magnet is charged by passing a momentary 220-A dc current through the charging coil encapsulated in the surrounding epoxy matrix. The one-piece piston and coil form (10-cm diam) carries 212 turns of AWG-30 copper wire and is suspended from a single neoprene circumferential seal. In spite of natural rubber's many desirable mechanical properties, this seal is made of neoprene because of its superior durability under the operating conditions of the high-temperature environment. Mechanical compliance of this seal was increased toward that of natural rubber by means of convolutions molded in the seal body. The piston (voice) coil is centered in the gap of the magnet by the center guide pin and Teflon bushing assembly, which serves also to counteract the buoyant force acting on the air-backed conical piston section. Front and rear mechanical stops prevent the piston from exceeding its maximum allowable displacement. The magnet gap and front cavity are filled with castor oil, which acts as a coupling medium to the water and provides the high acoustic impedance required at the periphery of the piston. The neoprene acoustic window provides a water-tight seal for the oil-filled cavity.

Changes in hydrostatic pressure acting on the piston are compensated by a passive pneumatic system, the heart of which is an elastic bag made of a butyl rubber compound whose permeability to water is very low. As the operating depth increases, the bag is compressed by the water head and increases air pressure behind the piston for compensation to depths of about 22 m.

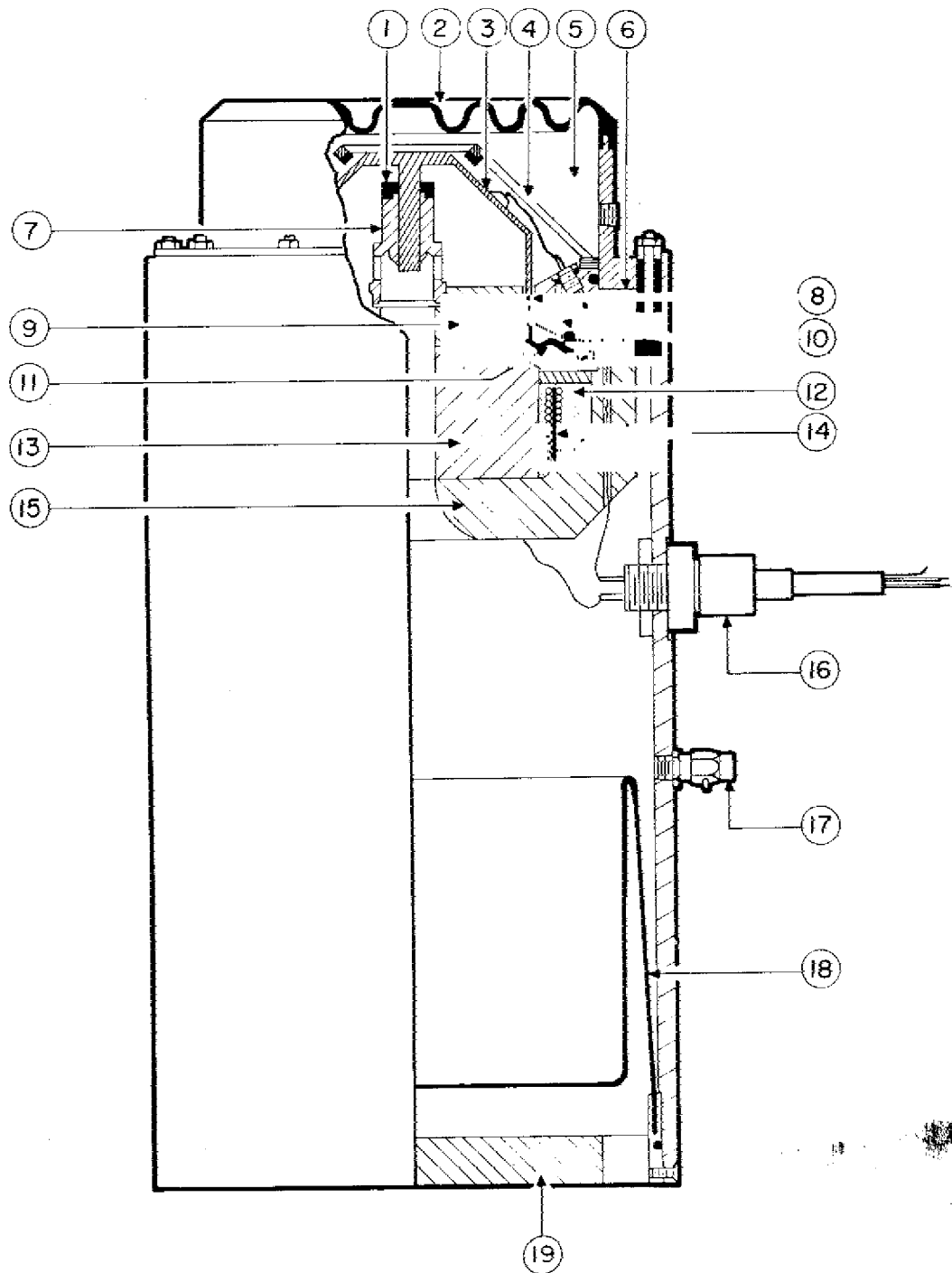


Fig. 3. Sectional view of USRD type J13 transducer: (1) rear mechanical stop, (2) corrugated neoprene acoustic window, (3) piston and coil form, (4) front mechanical stop, (5) oil-filled front cavity, (6) outer pole piece, (7) center guide pin and Teflon bushing assembly, (8) driving coil, (9) inner front pole piece, (10) oil flow holes, (11) neoprene circumferential seal, (12) lead-epoxy potting compound, (13) Alnico 5-7 magnet, (14) charging coil, (15) back pole piece, (16) waterproof electrical connector, (17) air filling valve, (18) compliant butyl rubber pressure-compensation bag, and (19) housing back plate.



velocities;  $Bli$  represents the force generated by the current-carrying coil moving in the magnetic gap.

Inspection of the equivalent circuit shows the importance of having a large case mass relative to that of the piston and the necessity for maintaining high acoustic impedance at the oil-filled slit and flow holes.

Several of the circuit elements are depth dependent. The compliances of the piston cavity  $C_1$ , compensation cavity  $C_2$ , and seal cavity  $C_3$  decrease as hydrostatic pressure increases, while the water mass in the compensation cavity increases with depth.

Among the simplifying assumptions made in the derivation of the equivalent circuit were, for example, the omission of all the effects of acoustic pressure in the water upon various parts of the transducer and the transformers necessary to couple two volume velocities to the compensation bag compliance and water mass. Also, the motion of the diaphragm was considered to be only that of a rigid piston.

The circuit in Fig. 4 is based on the classical or impedance analogy (voltage analogous to pressure, current analogous to volume velocity), which is inconvenient for the analytical description of a magnetic transducer. A more convenient version of the equivalent circuit for detailed analysis is the mobility analogy (voltage analogous to volume velocity, current analogous to pressure) shown in Fig. 5, wherein the electrical elements have been included and the transformers have been removed. The electroacoustical "turns ratio"  $N$  is determined by the transduction principle used and the dimensions of the radiators involved. The denominator

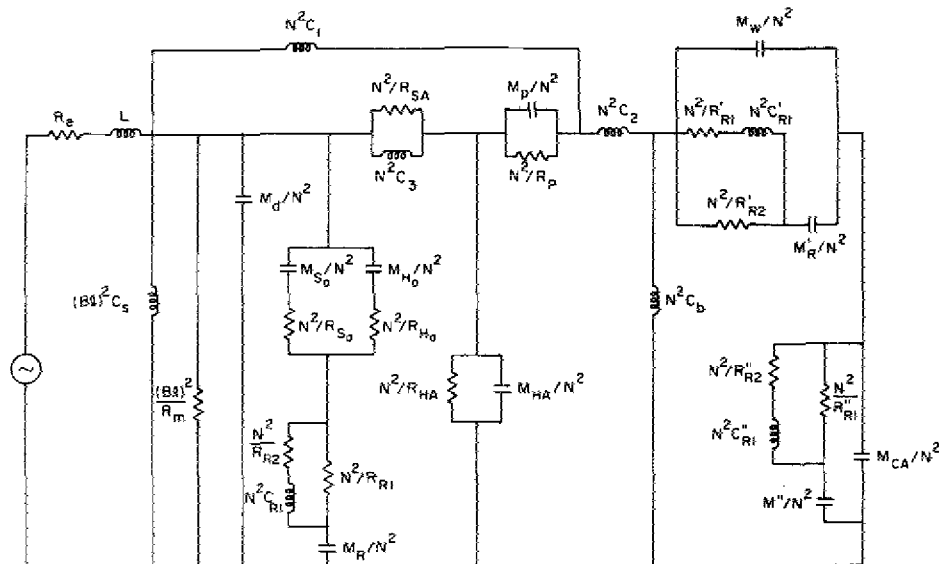


Fig. 5. Equivalent circuit for USRD type J13 transducer, mobility analogy;  $N^2 = (Bl)^2 / [A_2 - (A + A_1)]^2$ .

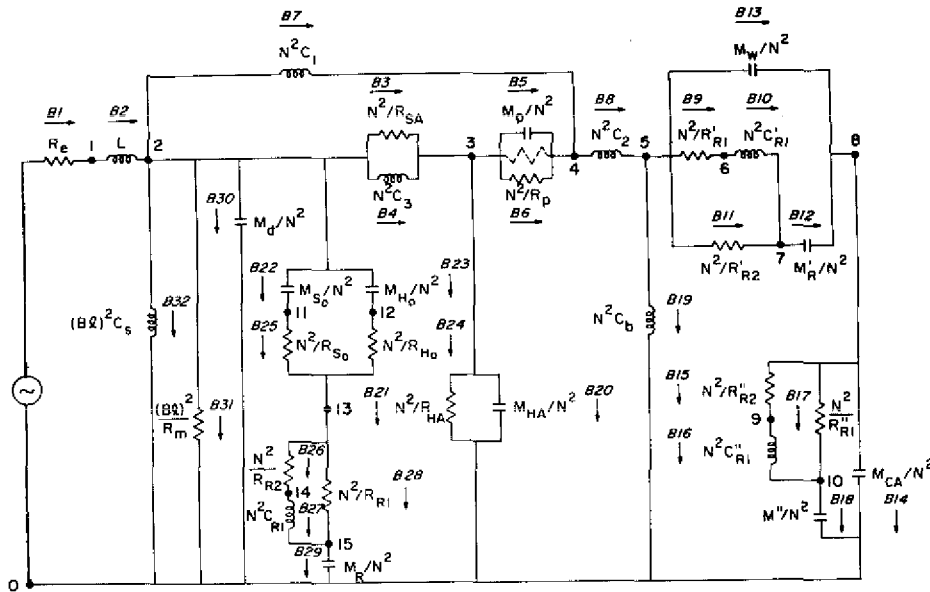


Fig. 6. Equivalent circuit for USRD type J13 transducer, mobility analogy for electronic circuit analysis by time-sharing computer program;  $N^2 = (Bl)^2 / [A_2 - (A + A_1)]^2$ .

of the "turns ratio" in Fig. 5 is derived from combination of the transformer ratios of the case (area  $A_2$ ) and the piston and seal (area  $A$  and  $A_1$ ) upon which forces of equal amplitude but opposite phase are acting.

The acoustic pressure generated by the piston at distance  $r$  can be obtained from

$$p = (1/r) (P_A \rho_0 c_0 R_\theta / \pi)^{1/2} \quad (6)$$

where  $P_A$  is the acoustic power output and  $R_\theta$  is the directivity factor.

At most frequencies in the range under consideration, calculation of the pressure generated at one meter can be simplified by setting the directivity factor in Eq. (6) equal to unity.

In terms of the equivalent electrical circuit, the acoustic power radiated by the piston is equal to the power dissipated in the radiation resistances  $N^2/R_{R1}$  and  $N^2/R_{R2}$ . If an input current of 1 A is specified, the transmitting current response can be represented by

$$p = (P_{RR} \rho_0 c_0 / \pi)^{1/2}, \quad (7)$$

where  $P_{RR}$  is the power dissipated in the radiation resistance.

Figure 6 shows the mobility analogy circuit with branches and nodes labeled in the format of the time-sharing computer program used for the

electronic circuit analysis. The dashed line shown between branches 5 and 6 represents the compressed metal-fiber acoustic resistors used at each end of the magnet passage to damp the resonance of the hole and piston cavity.

Values for the elements of the circuit were obtained by either direct measurement, calculation from measurements of motional impedances of the transducer under various loading conditions, or were computed. The values used and their derivations are outlined in Appendix A.

Because power dissipated in a branch can be selected as an output of the analysis program, the power dissipated in branches 26 and 28 represents the acoustic power radiated from the piston; and the power dissipated in branches 9, 11, 15, and 17 represents the acoustic power associated with the back and case radiation.

The transmitting current response obtained from the power dissipated in the radiation resistance branches and Eq. (7) is compared with the measured response of the transducer in Fig. 7. The apparent discrepancies between the measured and calculated results seen in these curves are largely attributable to the effects of the simplifying assumptions made in the circuit derivation and to the difficulties in assigning accurate values to some of the circuit elements. For example, resolution of the values obtained from the motional impedance measurements made at very low frequencies is, at best, only fair; and it is difficult, if not impossible, to measure or calculate values for the compensation cavity-compensation bag compliance combination under actual operating conditions. The positive slope of the curve for values measured between 1500 and 3000 Hz is caused by flexural resonances in the piston that would not be accounted for by calculated values because of the earlier assumption that the diaphragm moves as a rigid piston.

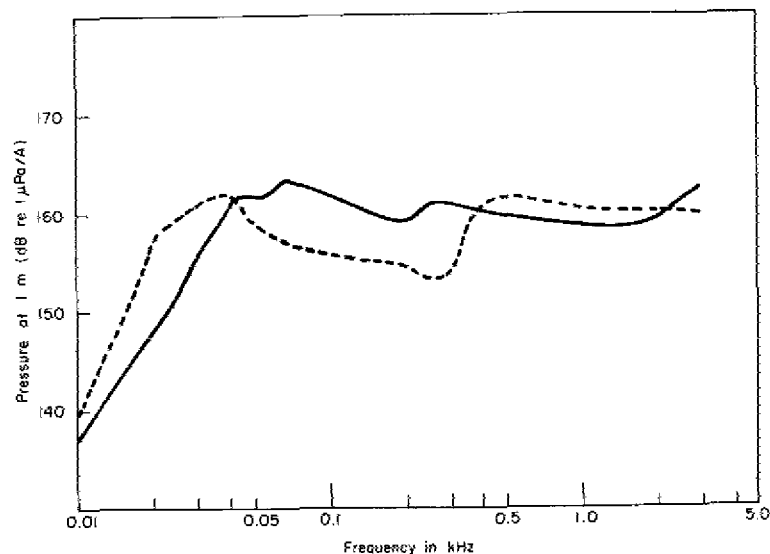


Fig. 7. Comparison of USRD type J13 transmitting current response data obtained by measurements (solid-line curve) with results from the equivalent circuit calculations (dashed-line curve).

## Conclusions

The USRD type J13 transducer, which is based on an old transduction principle, is a unique and adaptable underwater acoustic source. The J13 radiator, adapted in various configurations, fulfills a substantial portion of the underwater acoustic community's needs for low-audio-frequency sources. This transducer has been consistently in high demand since the time of its development.

## Acknowledgments

As is often the case in developing new hardware, it is difficult to single out any particularly deserving individual. The basic patent on this transducer is held by R. J. Kieser, J. R. Bass, and J. E. Donovan. Others who have made significant contributions include G. D. Hugus, L. E. Ivey, and S. H. Kazimir. Continuing design improvement has been pursued by Mr. Hugus and the author.

## References

- [1] C. C. Sims, "High-Fidelity Underwater Sound Transducers," Proc. IRE 47, 866 (1959).
- [2] L. L. Beranek, *Acoustics* (McGraw-Hill, New York, 1954), pp. 188-189.
- [3] L. E. Kinsler and A. R. Frey, *Fundamentals of Acoustics* (Wiley and Sons, New York, 1962), 2nd ed., Chap. 10.
- [4] E. Skudrzyk, *The Foundations of Acoustics* (Springer-Verlag, New York, 1971), pp. 348-354.
- [5] I. D. Groves, "Twenty Years of Underwater Electroacoustic Standards," NRL Report 7735, 21 Feb 1974, pp. 120-131 [AD-776 214].
- [6] A. M. Young, "Proposal for the Development of a High-Power, Low-Frequency Underwater Acoustic Source," NRL Memorandum Report 2897, 1 Nov 1974 [AD-A000 657].
- [7] Reference [2], pp. 128-139.

## Appendix A

### Determination of Values for Elements of the J13 Equivalent Circuit

#### General Considerations

Figure 6 of this report shows the branches and nodes of the J13 equivalent circuit in the notational format of the time-sharing computer program used for the electronic circuit analysis. All temperature- and pressure-dependent variables were computed for the temperature 20°C and the pressure equivalent to 15 m depth (150 kPa). In all cases, the symbol "a" refers to the radius of the circular aperture or surface under consideration.

#### Turns Ratios

The electromechanical "turns ratio" is  $B\ell$ , where  $B$  is the magnetic flux density in the magnet gap and  $\ell$  is the length of the current-carrying conductor interacting with  $B$ . The nominal value of  $B$  for the magnet assembly is  $1.2 \text{ Wb/m}^2$  and the nominal value for  $\ell$  is 66 m, which give a turns ratio value of 79.2 Wb/m. Results of repeated measurements of  $B\ell$  were between 78.5 and 80.0 Wb/m, which indicates that the nominal values are reasonably representative of the mean value.

The electroacoustical "turns ratio" is calculated from

$$N = B\ell/[A_2 - (A + A_1)],$$

where  $A$  is the cross-sectional area of the piston,  $A_1$  is the area of the circumferential seal-suspension member, and  $A_2$  is the cross-sectional area of the case. Substitution of the nominal dimensions  $A = 8.107 \times 10^{-3} \text{ m}^2$ ,  $A_1 = 4.560 \times 10^{-3} \text{ m}^2$ , and  $A_2 = 3.767 \times 10^{-2} \text{ m}^2$ , gives

$$N = 3.168 \times 10^3 \text{ Wb/m}^3.$$

#### Branches 1 and 2, Blocked Electrical Impedance

Range of electrical impedance measurements for blocked mechanical motion:

$$R: 24.5 \Omega \text{ at } 10 \text{ Hz to } 104.0 \Omega \text{ at } 3.0 \text{ kHz}$$

$$L: 0.0 \text{ H at } 10 \text{ Hz to } 2.7 \times 10^{-3} \text{ H at } 3.0 \text{ kHz}$$

#### Branch 3, Acoustic Resistance of Air Slit between Piston and Seal Cavities

$$R_{SA} = 12\eta\ell/t^3w,$$

where  $\eta$  is the viscosity coefficient for air,  $l$  is the width of the slit,  $t$  is the slit opening, and  $w$  is the mean circumference of the slit.

$$R_{SA} = 1.10 \times 10^6 \text{ kg/m}^4 \text{ s}$$

$$N^2/R_{SA} = 9.11 \ \Omega$$

#### Branch 4, Acoustic Compliance of Seal Cavity

$$C_3 = p_0 V_0 / \gamma p^2,$$

where  $p_0$  is the initial cavity pressure,  $V$  is the initial cavity volume,  $p$  is the pressure at operating depth, and  $\gamma$  is the ratio of specific heats for air.

$$C_3 = 6.67 \times 10^{-11} \text{ m}^5 / \text{N}$$

$$N^2 C_3 = 6.69 \times 10^{-4} \text{ H}$$

#### Branch 5, Acoustic Mass of the Magnet Passageway

$$M_P = \rho_0 (l + 2l') / \pi a^2,$$

where  $\rho_0$  is the density of the air,  $l$  is the passage length,  $l'$  is the end correction for the passage, and  $a$  is the radius of the passage.

$$M_P = 3.37 \times 10^2 \text{ kg/m}^4$$

$$M_P / N^2 = 3.35 \times 10^{-5} \text{ F}$$

#### Branch 6, Acoustic Resistance of the Magnet Passage

The acoustic resistance of the magnet passage is unimportant because its equivalent electrical resistance is shunted by the equivalent electrical resistance of the compressed metal fiber acoustic resistors at each end of the passage. The equivalent electrical resistance was determined from the difference in motional impedances measured with and without the resistors in the passage, yielding

$$N^2/R_P = 5.0 \ \Omega.$$

### Branch 7, Acoustic Compliance of the Piston Cavity

$$C_1 = P_0 V_0 / \gamma P^2 = 2.87 \times 10^{-10} \text{ m}^5 / \text{N}$$

$$N^2 / C_1 = 2.88 \times 10^{-3} \text{ H}$$

### Branch 8, Acoustic Compliance of the Compensation Cavity

Although it is clearly not a rigid chamber, the compensation cavity  $C_2$  is treated as if it were; closure to the water is effected by the rubber compensation bag. Unlike the piston and seal cavity compliances, the volume is allowed to decrease with increasing hydrostatic pressure.

$$C_2 = 4.02 \times 10^{-9} \text{ m}^5 / \text{N}$$

$$N^2 C_2 = 4.04 \times 10^{-2} \text{ H}$$

### Branch 9, Radiation Resistance, Back Radiation

Back radiation is transmitted through two  $1.905 \times 10^{-2}$ -m-diam holes in the rear of the case, mechanically in parallel.

$$R'_{R1} = 0.504 \rho_0 c / \pi a^2 = 1.326 \times 10^9 \text{ kg/m}^4 \text{ s},$$

where  $c$  is the speed of sound in water.

$$N^2 / R'_{R1} = 7.57 \times 10^{-3} \Omega$$

### Branch 10, "Radiation Compliance," Back Radiation

For two  $1.905 \times 10^{-2}$ -m-diam holes, mechanically in parallel,

$$C'_{R1} = 5.44 a^3 / \rho_0 c^2 = 1.042 \times 10^{-15} \text{ m}^5 / \text{N}$$

$$N^2 C'_{R1} = 1.049 \times 10^{-8} \text{ H}$$

### Branch 11, Radiation Resistance, Back Radiation

For two  $1.905 \times 10^{-2}$ -m-diam holes, mechanically in parallel,

$$R'_{R2} = \rho_0 c / \pi a^2 = 2.631 \times 10^9 \text{ kg/m}^4 \text{ s}$$

$$N^2 / R'_{R2} = 3.816 \times 10^{-3} \Omega$$

### Branch 12, Radiation Mass, Back Radiation

For two  $1.905 \times 10^{-2}$ -m-diam holes mechanically in parallel,

$$M'_R = 0.1952 \rho_0 / a = 4.098 \times 10^4 \text{ kg/m}^4$$

$$M'_R / N^2 = 4.082 \times 10^{-3} \text{ F}$$

### Branch 13, Acoustic Mass of Water in Compensation Bag Housing

$$M_{WA} = (V_c - p_0 V_0 / p_d) / (\pi a^2)^2,$$

where  $V_c$  is the volume of the housing,  $p_0$  is the initial pressure,  $V_0$  is the volume of the bag,  $p_d$  is the pressure at operating depth, and  $\pi a^2$  is the cross-sectional area of the housing.

$$M_{WA} = 6.89 \times 10^3 \text{ kg/m}^4$$

$$M_{WA} / N^2 = 6.86 \times 10^{-4} \text{ F}$$

### Branch 14, Acoustic Mass of the Case

$$M_{CA} = M_m / A^2,$$

where  $M_m$  is the measured mass of the case and  $A^2$  is the cross-sectional area of the case.

$$M_{CA} = 3.88 \times 10^4 \text{ kg/m}^4$$

$$M_{CA} / N^2 = 3.86 \times 10^{-3} \text{ F}$$

### Branch 15, Radiation Resistance, Case Radiation

$$R''_{R2} = \rho_0 c / \pi a^2 = 3.984 \times 10^7 \text{ kg/m}^4 \text{ s}$$

$$N^2 / R''_{R2} = 0.252 \text{ } \Omega$$

Branch 16, Radiation Compliance, Case Radiation

$$C_{R1}'' = 5.44a^3/\rho_0 c^2 = 3.174 \times 10^{-12} \text{ m}^5/\text{N}$$

$$N^2/C_{R1}'' = 3.187 \times 10^{-5} \text{ H}$$

Branch 17, Radiation Resistance, Case Radiation

$$R_{R1}'' = 0.504\rho_0 c/\pi a^2 = 2.008 \times 10^7 \text{ kg/m}^4 \text{ s}$$

$$N^2/R_{R1}'' = 0.500 \text{ } \Omega$$

Branch 18, Radiation Mass, Case Radiation

$$M_R'' = 0.1952\rho_0/a = 1.783 \times 10^3 \text{ kg/m}^4$$

$$M_R''/N^2 = 1.776 \times 10^{-4} \text{ F}$$

Branch 19, Acoustic Compliance of the Compensation Bag

This is difficult, if not impossible, to measure or calculate. Values ranging from  $10^{-6}$  to  $10^2$  H were substituted in the circuit to arrive at the value  $7.0 \times 10^{-3}$  H. In effect, this says the bag is considerably more compliant than either of the closed cavities, but less compliant than the compensation chamber.

Branch 20, Acoustic Mass of Air Flow Holes in Outer Pole Piece

For eight holes, mechanically in parallel,

$$M_{HA} = 8\rho_0 \ell/\pi a^2 = 3.019 \times 10^3 \text{ kg/m}^4,$$

where  $\ell$  is the length of the holes.

$$M_{HA}/N^2 = 3.007 \times 10^{-4} \text{ F}$$

Branch 21, Acoustic Resistance of Air Flow Holes in Outer Pole Piece

For eight holes, mechanically in parallel,

$$R_{HA} = [\rho_0/8(\pi a^2)] [(2\omega\mu)^{1/2}(\ell/a + 2)],$$

where  $\omega$  is the angular frequency,  $\mu$  is the kinematic coefficient of viscosity, and  $\ell$  is the length of the hole.

$$R_{HA} = 4.456 \times 10^{-2} \text{ kg/m}^4 \text{ s},$$

calculated at 250 Hz and assumed to be constant.

$$N^2/R_{HA} = 2.254 \times 10^8 \Omega$$

#### Branch 22, Acoustic Mass of the Oil-Filled Slit at the Piston Periphery

$$M_{So} = 6\rho_0 \ell / 5wt,$$

$$M_{So} = 2.233 \times 10^5 \text{ kg/m}^4$$

$$M_{So}/N^2 = 2.225 \times 10^{-2} \text{ F}$$

#### Branch 23, Acoustic Mass of the Oil Flow Holes

For 46 holes,  $1.588 \times 10^{-3}$ -m diam, mechanically in parallel,

$$M_{Ho} = 46\rho_0 \ell / \pi a^2 = 1.022 \text{ kg/m}^4$$

$$M_{Ho}/N^2 = 1.018 \times 10^{-7} \text{ F}$$

#### Branch 24, Acoustic Resistance of the Oil Flow Holes

For 46 holes,  $1.588 \times 10^{-3}$ -m diam, mechanically in parallel,

$$R_{Ho} = 8\eta \ell / 46\pi a^4,$$

where  $\eta$  is the viscosity coefficient for castor oil and  $\ell$  is the length of the holes.

$$R_{Ho} = 3.056 \times 10^9 \text{ kg/m}^4 \text{ s}$$

$$N^2/R_{Ho} = 3.285 \times 10^{-3} \Omega$$

#### Branch 25, Acoustic Resistance of the Oil-Filled Slit at the Piston Periphery

$$R_{So} = 12\eta \ell / t^3 w,$$

where  $\eta$  is the viscosity coefficient for castor oil,  $\ell$  is the width of the slit,  $t$  is the slit opening, and  $w$  is the mean circumference of the slit.

$$R_{So} = 3.523 \times 10^{10} \text{ kg/m}^4 \text{ s}$$

$$N^2/R_{So} = 2.850 \times 10^{-4} \Omega$$

Branch 26, Radiation Resistance, Piston Radiation

$$R_{R2} = \rho_0 c / \pi a^2 = 1.829 \times 10^8 \text{ kg/m}^4 \text{ s}$$

$$N^2 / R_{R2} = 5.489 \times 10^{-2} \Omega$$

Branch 27, "Radiation Compliance," Piston Radiation

$$C_{R1} = 0.544 a^3 / \rho_0 c = 3.123 \times 10^{-14} \text{ m}^5 / \text{N}$$

$$N^2 / C_{R1} = 3.135 \times 10^{-7} \text{ H}$$

Branch 28, Radiation Resistance, Piston Radiation

$$R_{R1} = 9.219 \times 10^7 \text{ kg/m}^4 \text{ s}$$

$$N^2 / R_{R1} = 0.109 \Omega$$

Branch 29, Radiation Mass, Piston Radiation

$$M_R = 0.1952 \rho_0 / a = 3.700 \times 10^3 \text{ kg/m}^4$$

$$M_R / N^2 = 3.686 \times 10^{-4} \text{ F}$$

Branch 30, Acoustic Mass of the Diaphragm

This is measured statically and from "added mass" technique in which the shift in the frequency of mechanical resonance caused by a known mass is used to determine the *unknown* mass.

$$M_d = M_m / (\pi a^2)^2,$$

where  $M_m$  is the measured mass.

$$M_d = 1.375 \times 10^3 \text{ kg/m}^4$$

$$M_d / N^2 = 1.370 \times 10^{-4} \text{ F}$$

Branch 31, Mechanical Resistance of Diaphragm Suspension and Guide Bushing

The electrical equivalent is derived from motional impedance of magnet-diaphragm assembly measured in a vacuum.

$$(Bl)^2 / R_m = 73 \Omega$$

## Branch 32, Mechanical Compliance of Suspension-Seal Assembly

Actual value used is the combination of suspension-seal assembly and oil-filled front piston cavity compliances. Electrical equivalent is derived from measured motion impedance.

$$(Bl)^2 C_s = 0.619 H$$